JOURNAL OF QUATERNARY SCIENCE (2022) 1–12 ISSN 0267-8179. DOI: 10.1002/jqs.3471

JQS Journal of Quaternary Science QRA Quaternary Research Association

Rinikerfeld Palaeolake (Northern Switzerland) – a sedimentary archive of landscape and climate change during the penultimate glacial cycle

LUKAS GEGG,[1,2]* FLAVIO S. ANSELMETTI,[2] GAUDENZ DEPLAZES,[3] MARIA KNIPPING,[4] HERFRIED MADRITSCH,[3] DANIELA MUELLER,[1] FRANK PREUSSER,[1] HENDRIK VOGEL[2] and MARIUS W. BUECHI[2]

[1]Institute of Earth and Environmental Sciences, University of Freiburg, Albertstraße 23b, 79104, Freiburg, Germany
[2]Institute of Geological Sciences and Oeschger Centre for Climate Change Research, University of Bern, Baltzerstrasse 1+3, 3012, Bern, Switzerland
[3]National Cooperative for the Disposal of Radioactive Waste (Nagra), Hardstrasse 73, 5430, Wettingen, Switzerland
[4]Institute of Biology, University of Hohenheim, Garbenstraße 30, 70599, Stuttgart, Germany

Received 24 May 2022; Revised 25 July 2022; Accepted 31 July 2022

ABSTRACT: While timing and ice extent of the last glacial maximum are generally well known, the courses of earlier glaciations have remained poorly constrained, with one of the main reasons being the scarcity of sedimentary archives. This study introduces a new palaeolake record from a Mid-Pleistocene glaciofluvial channel system in the Lower Aare Valley (Northern Switzerland). The record of Rinikerfeld comprises a >40 m long succession of Quaternary deposits that are targeted by multi-method sedimentological analysis. Sedimentary facies together with geochemical and geotechnical parameters, pollen content, as well as luminescence ages allow the reconstruction of the establishment, evolution and infilling of the early Marine Isotope Stage 6-aged Rinikerfeld Palaeolake. A drastic change in lake sediment composition and structure indicates cessation of the initial glacially derived input, which is explained by landscape modification and drainage rerouting during the Penultimate (Beringen) Glaciation. Geochemical and palynological data further reveal cold, initially periglacial but slightly ameliorating, climate conditions, while the lake was progressively filled up by local runoff, before being buried by periglacial colluvial diamicts, and potentially overridden by ice. It is therefore concluded that the onset of the Beringen Glaciation was an environmentally as well as geomorphically dynamic time period in the Northern Alpine Foreland.

KEYWORDS: Northern Alpine foreland; palaeolake; penultimate glaciation; periglacial lake; sedimentary archive

Introduction

A profound knowledge of past environmental conditions is vital for projecting and mitigating future ecological changes and challenges (Tierney *et al.*, 2020). In the Alps and the Northern Alpine foreland, the recent past has been characterised by the repeated and extensive glaciations of the Pleistocene. Here, the ice advances of the last glacial cycle (Gaar *et al.*, 2019; Gribenski *et al.*, 2021; Ivy-Ochs *et al.*, 2008; Seguinot *et al.*, 2018), notably the last glacial maximum (LGM; Ivy-Ochs *et al.*, 2022; Kamleitner *et al.*, 2022; Starnberger *et al.*, 2011), are rather well constrained by field evidence and numerical dating. This does not, however, apply to the older glaciations of the Middle and Early Pleistocene, which are far more poorly understood. Not only their timing and extent, but also the number of ice advances that occurred throughout the Quaternary are still the subject of debate. While in the Eastern Alps, the fourfold glaciation scheme of Penck and Brückner (1909) is still successfully applied (Van Husen and Reitner, 2011), at least eight but potentially 15 or more extensive glaciations are postulated for the Swiss Alps (Preusser *et al.*, 2011; Schlüchter *et al.*, 2021).

One of the main reasons for these striking uncertainties and differences is the paucity and fragmentary nature of the sedimentary record. The remnants of pre-LGM glaciations have often been intensively weathered under periglacial and interglacial conditions, and/or eroded and obliterated by younger ice advances (Hughes *et al.*, 2019; Merritt *et al.*, 2019). In addition, deposits related to older glaciations can often be challenging to date (e.g. Lian and Roberts, 2006; Mueller *et al.*, 2020), and therefore to correctly classify and interpret. Some of the most valuable scientific archives of the Pleistocene consist of the deposits of ancient lakes that served as sediment sinks, and these archives may allow for detailed environmental reconstructions through sedimentological, geochemical and palynological studies. However, only few such records which predate the LGM are known from Switzerland (Anselmetti *et al.*, 2010; Buechi *et al.*, 2018; Dehnert *et al.*, 2012; Preusser *et al.*, 2005; Schlüchter, 1989; Schwenk *et al.*, 2022).

The focus of this study is the Rinikerfeld in central Northern Switzerland, where scientific drilling was conducted in the context of the Quaternary investigation programme of the Swiss National Cooperative for the Disposal of Radioactive Waste (Nagra). This drilling recovered a new, pre-LGM palaeolake record that is interpreted based on a multi-method sedimentological analysis.

Geological setting

The study area (Fig. 1) is located close to the present-day confluence of the rivers Aare, Reuss and Limmat, about 50 km northwest of the Alpine front, at the eastern margin of the Jura Mountains. The latter consist of Mesozoic carbonates, marls

*Correspondence: Lukas Gegg, as above.
Email: lukas.gegg@geologie.uni-freiburg.de

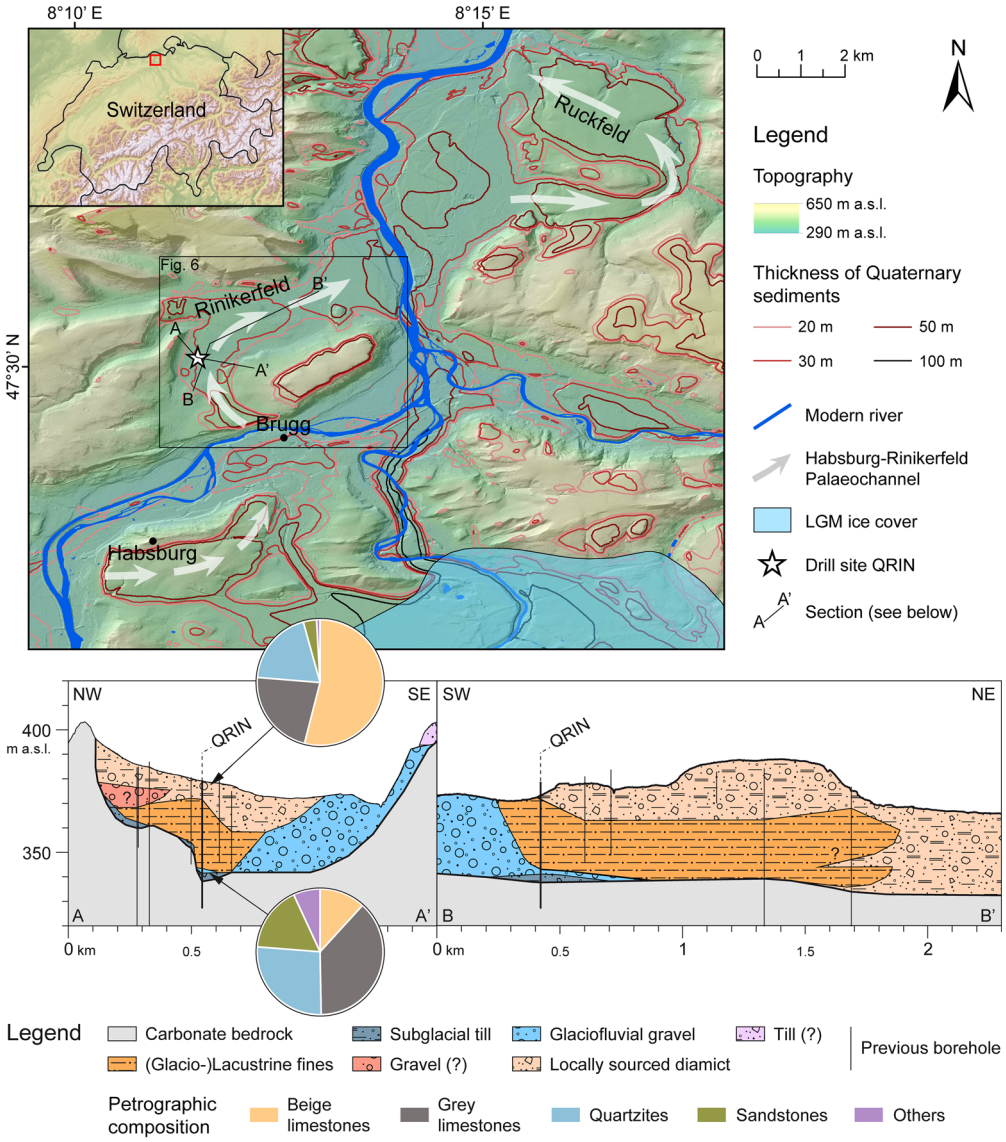

Figure 1. Top: Overview map of the study area with drill site QRIN. Thickness of Quaternary sediments taken from Loepfe R (2021, unpublished data; after Gegg *et al.*, 2021), Last Glacial Maximum ice cover after Bini *et al.* (2009). Bottom: Sections visualising the extent of the Rinikerfeld Palaeolake, based on borehole information (borehole logs from the database of Nagra projected onto profile lines over distances <500 m) and a local-scale geological map (Graf *et al.*, 2006). Pie charts illustrate the petrographic composition of coarse-grained deposits under- and overlying the palaeolake in QRIN. [Color figure can be viewed at wileyonlinelibrary.com]

and siliciclastics (Jordan *et al.*, 2008), were upthrusted in the Late Miocene (Burkhard, 1990; Looser *et al.*, 2021), and subsequently dissected by rivers (Ziegler and Fraefel, 2009). During the Pleistocene, glaciers developed in the Alps, expanded into the foreland and reached the study area several times (Preusser *et al.*, 2011). Advancing glaciers widened and locally overdeepened the river valleys (e.g. Gegg *et al.*, 2020, 2021) that progressively lowered over time due to repeated base level drops (Bitterli-Dreher *et al.*, 2007). Today, remnants of ancient, elevated valleys are mainly found in the shape of isolated occurrences of Early ('Deckenschotter'; Graf, 1993, 2009a), and of Middle Pleistocene gravel deposits ('Hochterrasse' system; Graf, 2009b).

The Habsburg–Rinikerfeld Palaeochannel (HRPC; Fig. 1) and its northward continuation via the Ruckfeld into the High Rhine Valley are, according to current interpretation, among the oldest Mid-Pleistocene landforms preserved in Switzerland ('Alte Rinnen'; Graf, 2009b). Accordingly, the HRPC is inferred to have formed during the Most Extensive Glaciation ('Möhlin Glaciation'; Dieleman *et al.*, 2022) and to have provided a pathway for glacier advances and glaciofluvial drainage until the Penultimate Glaciation ('Beringen Glaciation'; Graf, 2009b; Preusser *et al.*, 2011), before drainage was rerouted along the modern Aare Valley. Thus the HRPC hosts fluvial gravels (Hochterrasse) and glacigenic diamicts, but also fine-grained deposits interpreted as the product of local lake formation during the retreat of an early Mid-Pleistocene glaciation (Bitterli-Dreher *et al.*, 2007; Graf, 2009b). These fines, in the following referred to as deposits of the 'Rinikerfeld Palaeolake', have been observed in several boreholes north of the town of Brugg (Fig. 1), and are the target of the present study.

Methods

Scientific drilling

A >50 m long composite profile QRIN was compiled from two neighbouring boreholes in the Rinikerfeld (47°30′09″ N, 8°11′28″ E; see Gegg *et al.*, 2018). The drill cores, 10 cm in diameter, were recovered in plastic liners by a

combination of pneumatic hammering and wireline coring, allowing for excellent core quality, and transported to the Institute of Geological Sciences, University of Bern, for further processing. After core recovery and stepwise removal of the steel casing, a natural gamma log of the borehole was acquired with 5 cm depth resolution using a Century 9702 logging tool.

Initial core logging and sampling

Prior to core splitting, bulk gamma density and magnetic susceptibility were measured in 5 mm depth resolution using a Geotek Ltd multi-sensor core logger (Schultheiss and Weaver, null1992). One half of every split drill core was shielded from light to allow sampling for luminescence dating. Following line-scan imaging, detailed sedimentological descriptions were carried out. Where the sediment was sufficiently fine-grained, smear slides were prepared and bulk sediment samples were collected (~40 g of material) at sub-metre intervals for geochemical analysis. After sampling, the cores were archived at the core repository of Nagra).

Geochemical analysis

Water content was measured by weighing and freeze-drying the bulk sediment samples. Total inorganic carbon (TIC), total organic carbon (TOC), total sulphur, and total nitrogen were determined by flash-combustion of small (a few milligrams) sample amounts, combustion gas chromatography and gas analysis using a thermal conductivity detector. TIC was converted to $CaCO_3$ content by multiplication with a stoichiometric factor of 8.33. Selected sections of fine-grained deposits were further analysed with a Cox Ltd Itrax X-ray fluorescence (XRF) core scanner (Cr tube, 30 kV, 50 mA, 20 s integration time), using a protocol similar to the one described in Morlock *et al.* (2021), revealing relative element abundances in a resolution of 2500 μm, and of 500 μm in intervals of special interest.

Palynological analysis

Material of eight bulk sediment samples was further processed and analysed at the palynology laboratory at the Department of Molecular Botany, University of Hohenheim (Germany). Palynomorphs were extracted from the sediment by subsequent leaching with HCl, NaOH and HF, followed by chemical drying with acetic acid and acetolysis with acetic anhydride and H_2SO_4 (Eisele *et al.*, 1994). Tracer spores (*Lycopodium*) were added to each sample for calculating the pollen concentration. All samples were cleaned by ultrasonic sieving with a 7 μm mesh. In 2 cm^3 aliquots of the so-treated samples, pollen grains were identified under a microscope with 400× and 1000× magnification (Beug, 2004; Moore *et al.*, 1991), and the respective state of pollen preservation was noted.

Geotechnical analysis

During initial core logging, undrained shear strength was estimated with a pocket vane tester in metre intervals, and undisturbed whole-round core samples, ~20 cm in length, were collected for later analysis at the geotechnical laboratory of the Bern University of Applied Sciences in Burgdorf (Switzerland). To prevent drying and alteration, the samples were stored refrigerated and sealed prior to analysis. The preconsolidation pressure of sediment samples was determined by oedometer testing following ISO (2004). Horizontally oriented cylindrical samples (d = 50 mm, h = 20 mm) were cut out with a metal ring and placed in an oedometer chamber filled with deionised water. The samples were, under lateral confinement and enabled drainage, loaded with up to 3200 kN/m^2 in increments every 24 h. After every loading step, the compaction was measured, and the results evaluated following the work per unit volume approach by Becker *et al.* (1987). In addition, Atterberg Limits (liquid limit and plastic limit), i.e. the water content at which the material behaves mechanically in norm-specified ways, were determined after VSS (2008).

Luminescence dating

Previously, Mueller *et al.* (2020) reported results of luminescence dating of the QRIN profile: a total of eight samples had been obtained from the light-shielded half of the split cores, and sample preparation was conducted following standard laboratory procedures. Blue light stimulated luminescence measurements were performed on coarse- or fine-grained quartz, and infrared stimulated luminescence measurements on feldspar or fine-grained polymineral fractions. Four of the samples yielded finite quartz ages while six fading-corrected ages were derived for the feldspar or polymineral fractions (Mueller *et al.*, 2020). However, Mueller *et al.* (2020) have used a standard for calibration of the beta source in the luminescence reader that recently has been found to be erroneous regarding the assigned value (Autzen *et al.*, in press). Subsequently, the reader was recalibrated and the ages recalculated. The new recalculated ages are used here for further interpretation.

Results

Stratigraphy

Bedrock and basal diamictic deposits

Overlying grey calcareous marls of the Wildegg Formation, Effingen Member (Late Jurassic), at 337.6 m a.s.l., the composite profile QRIN comprises 41.2 m of Quaternary deposits (Gegg *et al.*, 2018), and is subdivided into five lithofacies associations (LFAs, Figs 2, 3). The succession begins with ~3.5 m of basal diamicts that are faintly bedded on a decimetre-scale (LFA 1, 41.2-37.6 m depth). They comprise angular to rounded clasts up to boulder size in a stiff silty matrix of grey-beige to brown colour. In the top half, the diamicts are generally matrix-supported and contain frequent striated clasts, whereas the bottom half is clast-supported but lacks striated clasts. The diamicts are overlain by poorly sorted sandy gravels with decimetre- to metre-scale beds that are frequently normally graded (LFA 2, 37.6-35.7 m depth). They are yellowish to brownish grey, with clasts occasionally covered in a coat of rusty brown (hydr-)oxides. Petrographically, LFAs 1 and 2 are dominated by grey limestones (~30–40%), quartzites (~20–30%) and sandstones (~15–20%; see Fig. 1).

Both diamicts and gravels are characterised by water content <10%, intermediate to high bulk densities (2.0-2.5 g/cm^3), and low to intermediate gamma signals (25-50 API). Magnetic susceptibility shows distinct peaks, likely due to individual coated clasts but also metal fragments broken off the core catcher, which are occasionally observed and create strong artificial peaks.

LFAs 1 and 2 are overlain by ~2 m of very diverse, predominantly sandy deposits (LFA 3, 35.7-33.5 m depth, Fig. 2A). They comprise faintly bedded sandy packages as well as horizontally laminated packages rich in silt and clay, and

massive diamictic interbeds containing clasts up to medium gravel size. LFA 3 is brown-beige with orange-brown and greyish sections. These deposits contain several layers with cemented nodules and, close to their base, clay chips. The entire section shows abundant signs of deformation and convolution. Water content ranges between 15 and 30%, and density around 2.0 g/cm^3, while gamma signals are elevated (~50 API), and magnetic susceptibility is generally low.

Horizontally laminated fines

Further up the succession, ~26 m of fine-grained deposits (LFA 4), predominantly silt and clay with occasional, often normally graded, sandy layers, can be subdivided into four subunits LFA 4a-d (Fig. 3). The lowermost ~2.5 m (LFA 4a, 33.5-31.1 m depth, Fig. 2B) are faintly horizontally laminated on a millimetre- to centimetre scale with decimetre-thick massive packages and sandy interbeds as well as individual, isolated fine gravel clasts. LFA 4a is brownish grey and locally intensively deformed resulting in a 'marbled' texture, which may be an original feature or drilling-induced. It is overlain by ~8 m of horizontally laminated, slightly sandy silts and clays with rhythmic bedding pattern of 2–3 cm thick olive-grey packages of ~1-10 mm laminae alternating with ~5 mm thick, finer-grained and darker beds (LFA 4b, 31.1-23.4 m, Fig. 2C). The deposits are occasionally interrupted by up to 10 cm thick, sandy interbeds. Above a sharp colour change at ~26.1 m from dark brownish grey to lighter ochre-grey, a second rhythmic pattern of 3–4 cm thick orange-brown horizontally laminated packages every ~10 cm is superimposed onto LFA 4b. These packages (LFA 4c, 26.1-9.3 m, Fig. 2D) become progressively thinner but occur in increasing frequency and finally supersede LFA 4b entirely at ~23.4 m below surface.

LFA 4c fines are more homogeneous, with lamina thicknesses of ~1 mm, and without a clear larger-order rhythmicity. While being orange-brown in an alternating sequence with LFA 4b, they are medium beige-grey in colour where they are vertically continuous (above ~23.4 m). Above ~16.3 m, four sub-metre intervals are observed where the deposits are of a strikingly dark grey to black colour that fades to orange-brown upon oxidation (Fig. 2E). These intervals are more faintly bedded, softer and wetter than the remainder of LFA 4c. Near the top, ~10 m below the surface, macroscopic plant

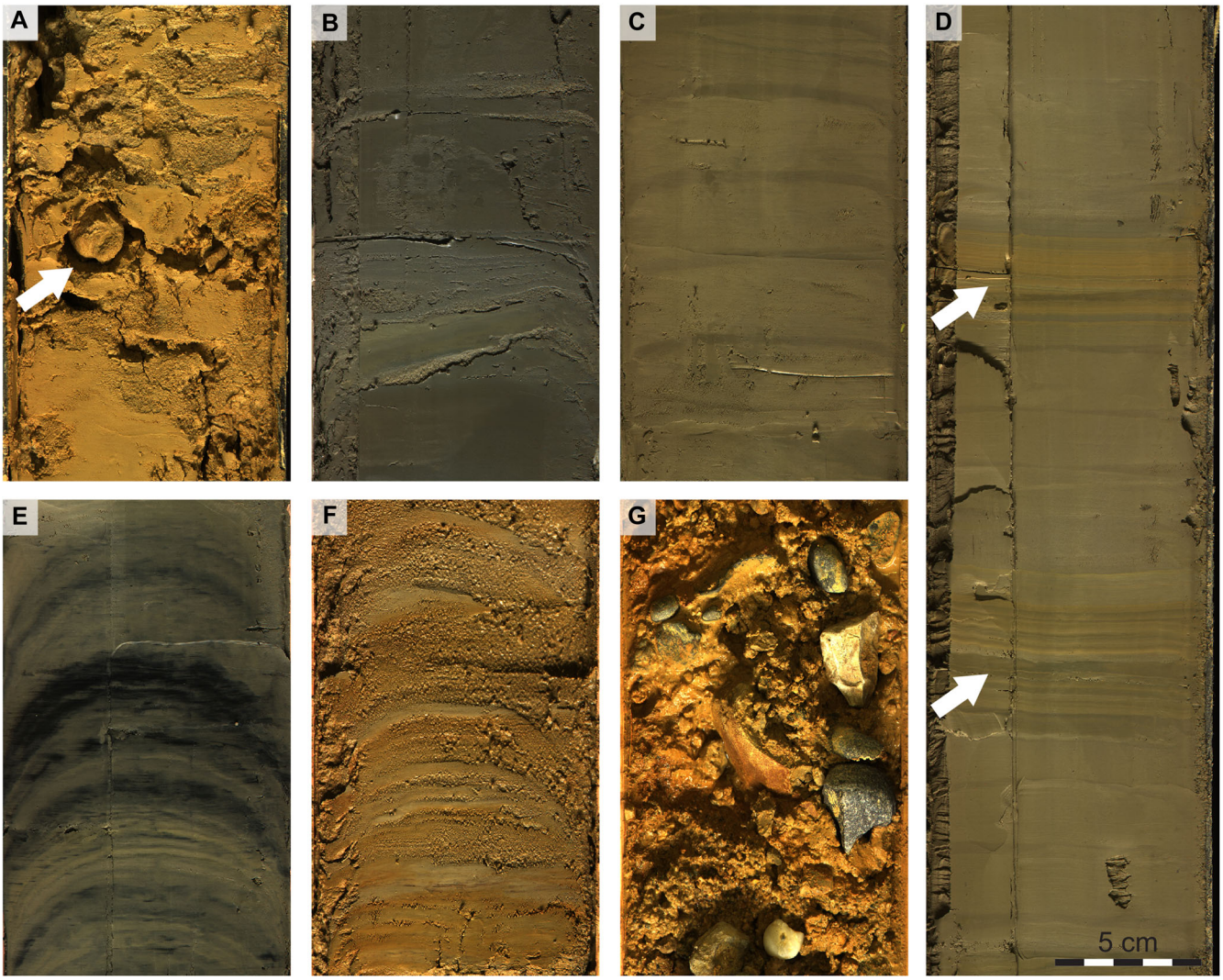

Figure 2. Core photos representing lithofacies associations (LFAs), width of all images is 10 cm. A: LFA 3, bedded clayey sand with cemented nodules and drilling-induced deformations (arrow; 34.0 m depth). B: LFA 4a, faintly bedded, sandy silt and clay with thin sand layers (31.2 m). C: LFA 4b, horizontally laminated silty clay with rhythmic bedding pattern (27.1 m). D: LFA 4b–4c transition: repeating orange-grey packages of LFA 4c (arrows) superimposed onto and, further upwards, gradually replacing LFA 4b sediments (see text; 25.5 m). E: LFA 4c, faintly laminated silty clay with occasional dark grey to black interbeds (15.8 m). F: LFA 4d, horizontally laminated, colourful alternation of sand with silt and clay (7.8 m). G: LFA 5, sandy diamict with rusty grain coatings (3.4 m). Note: basal diamicts of LFA 1 and overlying gravels of LFA 2 are not displayed. Note: photos of all core sections from QRIN are provided in Gegg *et al.* (2018). [Color figure can be viewed at wileyonlinelibrary.com]

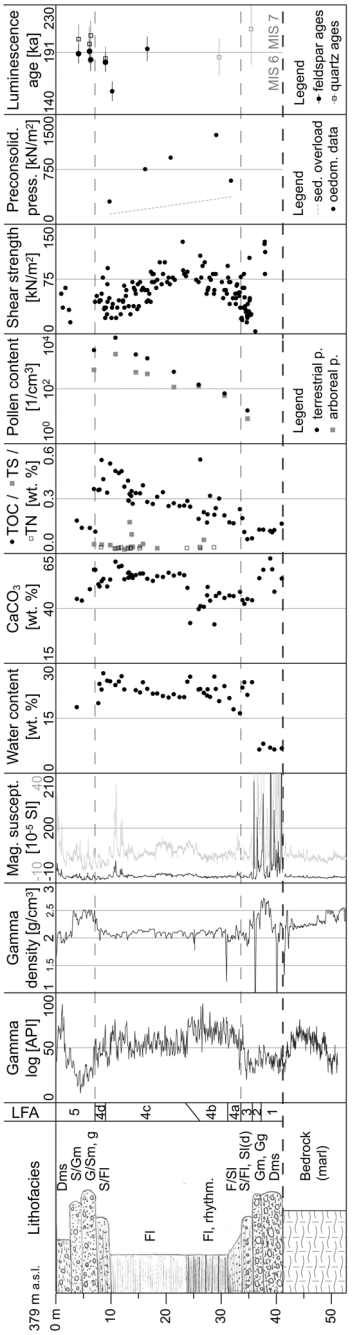

Figure 3. Composite plot of profile QRIN with various proxy data. Lithofacies codes refer to Eyles *et al.* (1983): F = fines, S = sand, G = gravel, D = diamicton, m = massive, g = normally graded, l = horizontally laminated, ms = matrix-supported and stratified, (d) = containing dropstones. For pollen composition, please refer to Table S1. Luminescence ages plotted in grey are minimum values (recalculated after Mueller *et al.*, 2020; see also Table S5).

fragments occur within a 30 cm thick, sandy intercalation. The uppermost ~2 m of fine-grained deposits are again more diverse (LFA 4d, 9.3-7.4 m, Fig. 2F) and consist of interbedded horizontally laminated and massive packages of clay, silt and sand with colours ranging from beige-grey to ochre-orange. At the very top, the sediment again contains macroscopic plant fragments as well as cemented sand nodules.

Fine-grained deposits of QRIN are characterised by intermediate density (2.0-2.2 g/cm^3), elevated gamma signal (50-70 API in LFA 4a/b, ~50 API in LFA 4c/d), and low magnetic susceptibility with only minor distinct peaks that correlate with dark layers in the upper LFA 4c. Water content is around 20-25%, and more homogeneous in LFA 4c/d, where a slight upward increase is observed, than in LFA 4a/b.

Cover diamicts

At the top of the profile, 7.4 m of predominantly beige to ochre-orange sandy diamicts are observed (LFA 5, Figs 2G, 3). These are matrix-supported and thick-bedded (decimetres) with normally graded packages. Clasts are predominantly beige limestones (~55%; plus ~25% and ~15% of quartzites and grey limestones, respectively; Fig. 1) up to coarse gravel size that are frequently angular, and occasionally covered by fine rusty coats. Towards the surface, the matrix becomes progressively more fines-rich and brown. The diamicts increase in gamma signal from ~25 to ~75 API from bottom to top, while density decreases from ~2.5 to ~2.0 g/cm^3, and magnetic susceptiblity remains generally low with only minor (low-intensity) peaks.

Geochemical signals

In the Rinikerfeld Palaeolake deposits, TOC increases gradually upcore from ~0.1 to ~0.5%. Both sulphur and nitrogen are detected in the upper parts of LFA 4b and LFA 4c/d, with maximum values below 0.2%. A sharp increase in $CaCO_3$ content from ~45 to ~55% is observed at the transition from LFA 4b to 4c (Fig. 3).

The elemental composition of the ~6 m long core section covering the transition from LFA 4b to 4c (23.1-28.7 m depth) was further investigated by XRF analysis (Fig. 4). Below ~26.1 m high-frequency variability occurs, but no systematic variations are observed within the rhythmically banded fine-grained deposits of LFA 4b. Only occasional sandy interbeds show increased Zr/Rb, and are relatively enriched in Si but depleted in K, Ti and Fe. Individual light and coarse-grained laminae are sharply enriched in Ca. The sudden colour change from dark brownish grey to lighter ochre-grey at 26.06 m coincides with an equally sudden drop in S content (Fig. 4). Above, distinctly Ca-enriched LFA 4c packages start to occur in alternating sequence with LFA 4b, and both Zr/Rb as well as Fe/Mn decrease (by ~50% and ~35%, respectively). The continuous LFA 4c interval at 23.4-23.1 m is rather homogeneous in elemental composition.

Pollen content

Throughout the lacustrine succession, a distinct trend of increasing pollen concentrations and species diversity is observed (Fig. 3, Table S1). LFAs 4a and 4b (33.5-23.4 m depth) contain only a few and likely largely reworked or allochthonous arboreal pollen (<10 grains per aliquot, projected to <150 grains per cm^3). In LFA 4c, starting at 21.39 m, pollen concentrations increase considerably (from ~400 up to >7000 grains per cm^3). However, throughout LFA

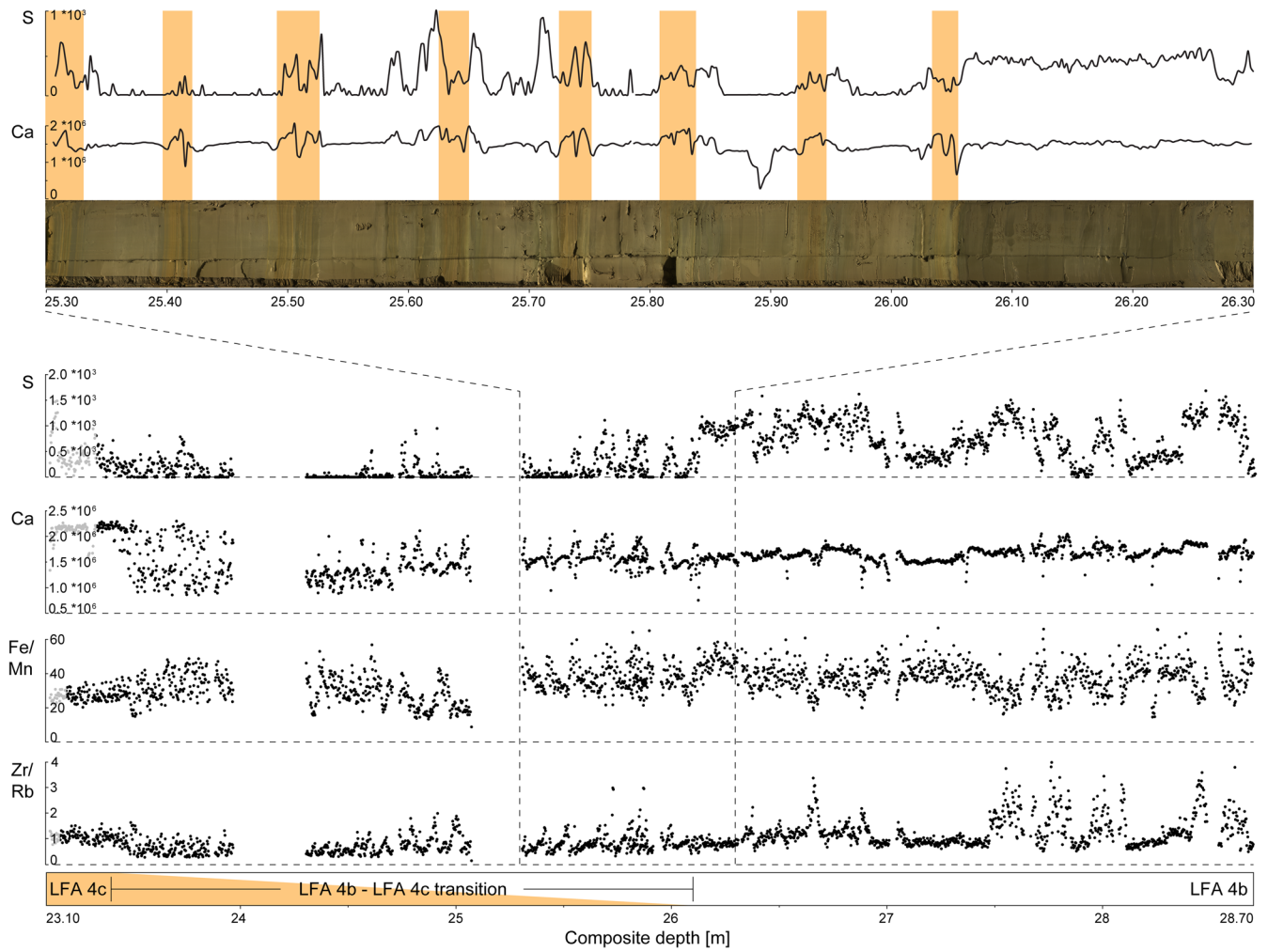

Figure 4. Selected XRF data of the upper lithofacies association (LFA) 4b and transition to LFA 4c (shaded orange), with zoom-in on drill core from 25.3-26.3 m depth (photograph). [Color figure can be viewed at wileyonlinelibrary.com]

4c, no more than ~25% arboreal pollen are encountered; instead, Poaceae and Cyperaceae occur in rather large numbers, as well as e.g. *Artemisia*, *Helianthemum*, *Thalictrum* and *Selaginella selaginoides* (see Table S1). Note: Cyperaceae are here included in the pollen sum due to frequently widespread occurrence in otherwise sparsely vegetated environments.

Geotechnical properties

The shear strength of Rinikerfeld Palaeolake deposits increases from ~20 kPa at the base of LFA 4 to ~130 kPa at the LFA 4b-4c boundary, but then decreases again to ~30 kPa at the top of LFA 4d (Fig. 3). Oedometer measurements of five samples were evaluated following the work per unit volume approach by Becker *et al.* (1987) and the results compared with the calculated sediment overload in the present-day setting (Table S2). Preconsolidation pressures exceeding sediment overload by >250% were determined for the intermediate three samples, and by 133 and 61% for the uppermost and lowest samples, respectively (Table S3; Fig. 3). It should be noted that the intermediate three samples were recovered by rotary drilling and both the uppermost and lowest samples by pneumatic hammering.

Six samples were tested for Atterberg Limits (liquid limit LL and plastic limit PL; Table S4), with the results plotted in Fig. 5. All samples plot above the A-line of Casagrande (1948), on or close to the T-line of glacial sediments (Boulton and Paul, 1976; Schlüchter, 1997; Trenter, 1999). The natural water content (WC) of all samples lies between LL and PL, with the exception of ATL-6, where WC is below the plastic limit

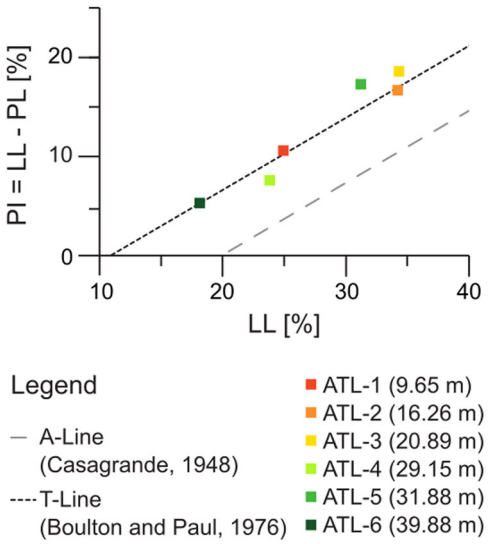

Figure 5. Plasticity diagram for the QRIN samples (see Table S4). PI = plasticity index. [Color figure can be viewed at wileyonlinelibrary.com]

(Table S4). Liquidity indices LI ((WC-PL)/(LL-PL)) range between 0.3 and 0.5 for all samples except ATL-6, where LI is -0.8.

Luminescence ages

For the lower part of the QRIN profile (including base of LFA 4b), only minimum ages corresponding to MIS 6 can be determined (Fig. 3; Mueller *et al.*, 2020). Samples taken from LFA 4c and LFA 4d gave luminescence ages of 159±8 ka to 194±10 ka and 186±10 ka, for the polymineral and quartz fractions, respectively (Table S5). Finite quartz ages for the top three samples from LFA 5 are between 198±14 ka and 205±12 ka, statistically consistent with fading-corrected feldspar ages of the same samples (185±9 ka to 192±10 ka).

Discussion

Local landscape and palaeolake evolution

At the base of the HRPC, glacigenic diamicts were recovered in QRIN (LFA 1). Their upper half is interpreted as a subglacial till as it frequently contains faceted and striated clasts shaped by glacial transport dispersed in a silty-sandy matrix (Evans *et al.*, 2006; Evans, 2007). The high density, the negative liquidity index, and the plasticity characteristics of the matrix (sample ATL-6 plotting on the T-line; Fig. 5) further support the interpretation as an overconsolidated till (Schlüchter, 1984). The petrographic composition dominated by grey limestones reflects an Alpine source, and the high abundance of quartzites further indicates that both the till and the overlying gravel (LFA 2) could be a correlative of the Habsburg Gravel (Graf, 2009b), the oldest glaciofluvial unit of the Hochterrasse system. Prior to the onset of lacustrine deposition, the gravel fill of the HRPC must have been dissected in order to create sufficient accommodation space (Fig. 1). Below the proper lake sediments, borehole QRIN encountered diverse sandy deposits (LFA 3, Fig. 2A). They are interpreted as the product of local reworking and redeposition in the newly formed topography, and their prominent brownish colour may be due to prolonged subaerial exposure, and thus a considerable hiatus between the inferred Habsburg Gravel and the Rinikerfeld Palaeolake.

According to the existing borehole data, the Rinikerfeld Palaeolake deposits extend over ~1.5 × 0.5 km^2, are ~26 m thick, and surrounded by Mesozoic bedrock and/or Pleistocene sediments (Fig. 1). At the distal northeastern end, they are bounded by diamictic deposits consisting mostly of locally sourced material that could represent a landslide body or fast-aggrading paraglacial debris fan, but potentially also a moraine ridge once damming the lake but no longer visible in the present-day topography (Figs 1, 6A). The lake deposits in QRIN start with ~2.5 m of rather faintly and thick-bedded fines with sand interbeds and, initially, few outsized gravel clasts (LFA 4a), which speaks for (glacio-)lacustrine sedimentation with small-scale mass wasting and traction currents. Together with presumed soft-sediment deformation features (although drilling-induced deformation cannot be excluded), this suggests a high sedimentation rate (Lister, 1984b; Mills, 1983; Pisarska-Jamrozy and Weckwerth, 2013). These deposits might be part of a glaciolacustrine delta.

Further up the succession (31.1-23.4 m depth; LFA 4b), the lacustrine fines are clay-dominated and well-bedded/horizontally laminated. A strikingly rhythmic pattern is observed, consisting of ~5 mm thick, finer-grained dark bands every 2-3 cm (Fig. 2C), which are not distinguished by XRF data. This indicates alternations in grain size only, suggesting an origin as detrital varves (Leonard, 1986; Zolitschka *et al.*, 2015) whose summer layers have been deposited in several sediment-input events, such as phases of increased snowmelt.

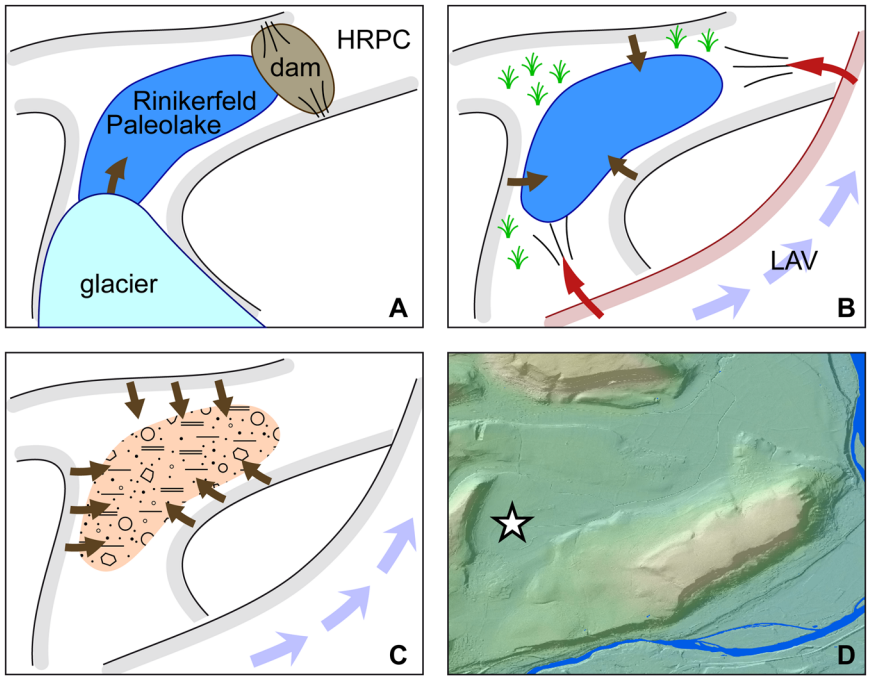

Figure 6. Schematic illustration of the inferred evolution of the Rinikerfeld. A: Around the MIS 7-6 boundary, a glacier advanced along the pre-existing Habsburg–Rinikerfeld Palaeochannel (HRPC). In front of this glacier, a lake developed in the Rinikerfeld, dammed by a sediment body, likely a landslide, and fed by meltwater (arrow). Deposition of LFA 4a,b during ice retreat. B: After glacial abandonment of the Rinikerfeld, a new channel was incised towards the southeast (modern Lower Aare Valley (LAV); flank drawn in red), and drainage rerouted. The Rinikerfeld Palaeolake was then mainly fed by local runoff (brown arrows) and occasionally reached by overspilling floods from the LAV (red arrows). Deposition of LFA 4c,d with pollen content suggesting the presence of open vegetation. C: After silting up, the lake was covered by colluvial diamicts (LFA 5), probably under periglacial conditions during MIS 6. D: Present-day situation (see Fig. 1 for orientation). Note: Larger-scale paleogeographic reconstructions have been presented by Graf (2009b). [Color figure can be viewed at wileyonlinelibrary.com]

This interpretation further suggests a sedimentation rate of few centimetres per year, corresponding to deposition of this lacustrine section over not more than a few hundred years. The dark olive-grey colour and homogeneous facies of LFA 4b supports a high sedimentation rate-setting with little oxygen exposure of sediments prior to burial (Anderson, 1985; Lister, 1984a; Van Dijk *et al.*, 1978), for example due to the lake being fed by turbid meltwater ('glacial milk').

The LFA 4b-4c transition is characterised by an increasing $CaCO_3$ content (~45 to ~55%), and a concurring decrease in Zr/Rb indicates a drop in clay mineral content (cf. Dypvik and Harris, 2001), as can also be inferred from the gamma log (Figs 3, 4). This indicates an essential change in sediment input that could represent a transition from an (indirectly) glacier-fed towards a more locally dominated lake, fed by runoff from the limestones and calcareous marls of the Jura Mountains (cf. Karlén and Matthews, 1992). This transition could be explained by an abandonment of the HRPC by the previously occupying glacier, and drainage rerouting into a new channel, which would likely involve a sharp decrease in sedimentation rate (cf. Regnéll *et al.*, 2019; Svendsen *et al.*, 2019). The modern Lower Aare Valley would be the most plausible candidate for this new channel (see Figs 1, 6B). It should be noted, however, that Atterberg Limits throughout the entire palaeolake plot close to the T-line (Fig. 5), and thus indicate a high degree in glacially derived material.

LFA 4c first occurs in the shape of repeating, orange-brown horizontally laminated packages a few centimetres thick starting at 26.1 m depth (Fig. 2D), which could represent more oxygenated conditions that became more frequent, and lastly continuous, at 23.4 m depth. This may be explained by the assumed lower sedimentation rate, or by decreasing water level and/or stratification of the lake (Moscariello *et al.*, 1998; Wennrich *et al.*, 2014). Increased oxygenation is supported by a slight decrease in Fe/Mn (Naeher *et al.*, 2013; Żarczyński *et al.*, 2019) and might explain in part the observed drop in S content (Fig. 4; Holmer and Storkholm, 2001). The sediments of LFA 4c are horizontally laminated with alternating lighter and darker layers that are significantly finer and less uniform than in LFA 4b, and that are interpreted as varves but with a lower and more variable sedimentation rate in the order of a few millimetres per year. Individual layers can be olive-grey or brownish, indicating variable oxygen exposure (Van Dijk *et al.*, 1978). Occasional intercalated sand layers indicate higher-energy sedimentation events of different origins. Individual coarser interbeds rich in Ca may have been deposited in response to heavy local rainfall or snow melt. Siliceous sand layers point towards a more distal sediment source, and are indicative of deposition of material derived from the Alps. Assuming that the HRPC was abandoned in favour of the modern Lower Aare Valley during deposition of the palaeolake succession, it is not unlikely that the Rinikerfeld became part of the Aare's floodplain and was occasionally inundated by overbank floods that delivered sediments from the Alpine catchment (Fig. 6B; Asselman and Middelkoop, 1995; He and Walling, 1998; Huybrechts, 2000). Alternatively, siliceous material may have also been washed in from smaller exposures of Neogene Molasse deposits southeast of the Rinikerfeld (Graf *et al.*, 2006).

At ~10 m below the surface, the lacustrine fines become more diverse, with horizontally laminated and massive packages of clay, silt and sand, and colours ranging from beige-grey to ochre-orange (LFA 4d, Fig. 2F). This marks the transition from a now silted-up lake basin to a shore setting, whose deposits may periodically have been subaerially exposed (Urban and Bigga, 2015). The inferred sedimentation rates of initially a few centimetres per year (LFA 4b), and later a few millimetres per year (LFA 4c) indicate a minimum 'lifetime' of the Rinikerfeld Palaeolake of a few thousand years.

The sediments of the Rinikerfeld Palaeolake are finally overlain by 7.4 m of thick-bedded matrix-supported diamicts whose petrographic spectrum consists of >50% light limestones derived locally from the Mesozoic rocks of the Jura Mountains. These diamicts contain predominantly angular clasts without striations and are very sandy but poor in silt and clay, which makes both a pure fluvial and a pure glacial origin implausible. Together, these characteristics are indicative of periglacial slope deposits (PSDs), i.e. the products of frost cracking, cryoturbation, solifluction and/or debris flows (Raab *et al.*, 2007; Veit *et al.*, 2017). Compared with last-glacial PSDs (Mailänder and Veit, 2001), those of the Rinikerfeld are strikingly thick, suggesting intensive subaerial erosion and redeposition of older unconsolidated sediments but probably also of local bedrock during the time of their formation (Fig. 6C).

Preconsolidation pressures determined for five sediment samples of the Rinikerfeld Palaeolake are significantly higher than the present-day overload (Fig. 3, Table S3). The three intermediate samples, recovered by wireline coring, show preconsolidation pressures that exceed their overload by >500 kN/m^2 or >250%. These values can be explained by overconsolidation under >20/40 m of dry/water-saturated sediment that has since been eroded, or >50 m of (static) glacier ice (O'Regan *et al.*, 2016; Van Gelder *et al.*, 1990). The topmost (9.65 m) and lowermost samples (31.88 m), recovered by pneumatic hammering, exceed the respective overload by ~200 kN/m^2 or 60-130%, corresponding to ~10/20 m of dry/water-saturated sediment or ~20 m of glacier ice. The overconsolidation recorded in the lacustrine deposits is enigmatic. Loading under a later ice advance cannot be excluded, and the irregular top surface of the Rinikerfeld Palaeolake deposits (Fig. 1) could point towards a phase of glacial overriding and erosion. However, neither sedimentological indication for overriding by ice (e.g. ice-contact deposits, glaciotectonism, fluid-escape structures; O'Regan *et al.*, 2016; Van der Meer *et al.*, 2009), nor potential gaps in the seemingly continuous Quaternary succession can be identified. It appears possible that the overconsolidation is a result of drying out, or of freezing and thawing of the sediment (Qi *et al.*, 2006), which could also account for the shear-strength pattern that shows a distinct peak at the LFA 4b/4c boundary (Fig. 3), where water levels may have been fluctuating, and generally lower.

Climatic and environmental change

The Pleistocene succession of QRIN starts with coarse-grained sediments, including a subglacial till, overlying pre-Quaternary bedrock. These are evidence for pleniglacial conditions during the Mid-Pleistocene. They are overlain, potentially with a significant hiatus in-between, by the Rinikerfeld Palaeolake that is identified as a cold, i.e. glacial/stadial, lake. This interpretation is based on the excellent preservation of the sedimentary lamination, the lack of macrofossils (throughout most of the succession, see below) and authigenic calcite as well as the generally low TOC values (max. ~0.5%; Fig. 3; Anselmetti *et al.*, 2010; Dehnert *et al.*, 2012; Vogel *et al.*, 2010). In addition, individual outsized clasts occurring at the very base of the lacustrine fines are interpreted as dropstones deposited in a lake that was initially in contact with glacier ice.

A distinct upward-increasing trend in TOC in the Rinikerfeld Palaeolake illustrates slightly ameliorating climate conditions (Fig. 3). Above ~16.3 m depth, dark grey to black intervals

occur that, when exposed to air, quickly fade to a rusty brown, which indicates that the colour is due to finely dispersed sulphides (Rickard *et al.*, 2017). These intervals thus provide the first visible indications for organic matter, but possibly also for mild bioturbation as they are much more faintly bedded than the remainder of LFA 4c (Berner, 1985; Suits and Wilkin, 1998). They are overlain by macroscopic plant fragments occurring ~10 and 7.4 m below the surface as indicators of vegetation cover in the vicinity.

This trend towards more temperate conditions is also evident from the pollen content of the lake deposits that strongly increases upwards (Fig. 3, Table S1). Low numbers of mostly arboreal taxa in LFA 4a and 4b are likely reworked and/or allochthonous (Sidler, 1984), and a consequence of the presumed high sedimentation rates of a few centimetres per year. In LFA 4c, the pollen spectra indicate an open steppe-tundra (cf. Starnberger *et al.*, 2013) that becomes progressively more diverse. No more than ~25% arboreal pollen are encountered throughout LFA 4c, and light-demanding taxa such as *Artemisia, Botrychium, Hippophae, Selaginella selaginoides*, Plumbaginaceae and a lot of Poaceae and Cyperaceae further support a continuously open vegetation with small shrubs (e.g. *Salix, Juniperus*; Lang, 1994; Oberdorfer, 1990). The presence of *Hippophae* and *Selaginella selaginoides* suggests summer temperatures as high as 10–15°C (Kolstrup, 1980), and individual findings of *Batrachium* and *Sparganium* types as well as *Botryococcus* and *Pediastrum* indicate the presence of a sparse swamp and aquatic flora (Table S1).

A thick cover of PSDs overlying the palaeolake succession finally indicates a second shift in climatic conditions, again towards a colder and probably vegetation-free environment. Although the according sedimentary evidence is lacking, the observed overconsolidation of the lake sediments could even be the result of a renewed ice advance overriding the site of QRIN.

Chronology and correlation

Luminescence ages of at least the upper 17 m of the Rinikerfeld profile indicate a rapid transition from a lacustrine to a colluvial-dominated periglacial environment at the transition of MIS 7-6 (Fig. 3), i.e. representing an early stage of the Penultimate (Beringen) Glaciation (Preusser *et al.*, 2011). For the lower part of the succession, only minimum age estimates were derived suggesting that those glacial to proglacial diamicts are of similar age to, or older than, the top units (Mueller *et al.*, 2020). Sedimentological evidence indicates that the entire palaeolake succession represents a single, short deposition phase in the order of a few thousand years. The deposits reflect a pronounced cold phase near the MIS 7-6 transition, followed by climatic amelioration and at least one further cold phase during the Penultimate (Beringen) Glaciation (see previous section), which is in good agreement with previous findings (e.g. Lowick *et al.*, 2015; see also below).

The Rinikerfeld Palaeolake could therefore be coeval with the lower part (Formation D–E) of the Bülach Trough infill (~25 km to the east; Buechi *et al.*, 2018). The latter consists of a basal till that is attributed to the MIS 6 and represents an ice advance excavating the overdeepened trough. This till is overlain by a retreat sequence of glaciodeltaic sands and glaciolacustrine fines and by a second stack of tills and basin fines suggesting a renewed extensive glaciation and retreat. This two-phase succession is truncated by a third, late Beringen ice advance (Buechi *et al.*, 2018). Similar findings have been reported from the Wehntal trough (~15 km to the east; Anselmetti *et al.*, 2010; Dehnert *et al.*, 2012), where an early Beringen waterlain till (Unit B; Dehnert *et al.*, 2012) is overlain by horizontally laminated, proglacial lacustrine fines with frequent dropstones that become progressively rarer, and later by increasingly sandy sediments containing sparse evidence for organic matter (Units C–E; Dehnert *et al.*, 2012). Analogous to the Bülach Trough, they are in turn overlain by the remnants of a later MIS 6 advance, as well as deposits of the last glacial cycle. Besides reworked palynomorphs, the lake deposits C–E of Wehntal sparsely contain pollen of cold-resistant trees and shrubs as well as upland herbs (Anselmetti *et al.*, 2010; Dehnert *et al.*, 2012). Despite the very different topographic settings, the successions of the Rinikerfeld Palaeolake on the one hand, and of the Wehntal and Bülach troughs on the other, are thus remarkably similar in their palaeoenvironmental evolution.

However, similarities are also observed with other Pleistocene records of the Alps and their northern foreland. Comparable (peri-)glacial lake deposits with pollen assemblages characterised by low concentrations of (far-travelled) conifer pollen and, later, increasing numbers of heliophile herb taxa have repeatedly been encountered in the basal parts of further (palaeo-)lakes. This includes records post-dating those of Rinikerfeld such as Baumkirchen (Barrett *et al.*, 2017, 2018), Lake Zurich (Lister, 1984a; Sidler, 1984) and Uster (Wyssling and Wyssling, 1978), but also older records such as Meikirch (Preusser *et al.*, 2005; Welten, 1982), Neusillersdorf (Fiebig *et al.*, 2014) and the Early Pleistocene 'Formation inférieure d'Ecoteaux' (Pugin *et al.*, 1993). Another presumably very similar deposit are the pre-MIS 6 Varves of Thalgut, which cannot be palyno-stratigraphically classified, according to Schlüchter (1989), due to their glacial character and paucity of pollen (see also Preusser and Schlüchter, 2004). Accordingly, it can be concluded that, while characteristic for an incipient ice-retreat phase, the pollen record, and sedimentary succession in general, of the Rinikerfeld Palaeolake are not stratigraphically distinct.

Conclusions

The succession of QRIN provides a new record of local landscape and environmental change during the onset of the Penultimate (Beringen) Glaciation. It represents the establishment and evolution of the Rinikerfeld Palaeolake within the previously glacial–glaciofluvial setting of the HRPC, reflecting the abandonment of said palaeochannel in favour of the modern, presently ~50 m lower-lying, Lower Aare Valley. This abandonment marks the transition from the Mid-Pleistocene to the Late Pleistocene terrace systems. In accordance with previous studies, the sedimentological, geochemical and palynological data further illustrate an amelioration of the initially cold conditions, followed by another climatic degradation as indicated by the deposition of periglacial colluvial deposits. The present study paints the picture of a Penultimate Glaciation whose early stages were associated with i) dynamically changing climate conditions (stadial–interstadial–stadial?), and ii) geomorphic activity in the shape of major drainage pathway rearrangement in the Northern Alpine foreland. In addition, it highlights the significance of lacustrine records as palaeoenvironmental archives of regional importance.

Acknowledgements. This study was funded by the Swiss National Cooperative for the Disposal of Radioactive Waste (Nagra). We would also like to kindly thank J. Krbanjevic for performing geochemical analyses, F. Nyffenegger for guidance during geotechnical analyses, A. Kuster and D. Schmid for support in the laboratory, as well as M.

Schwenk and Y. Tomonaga for company and support at the drill site. Finally, this manuscript benefited from constructive reviews by G. Monegato and J. Winsemann, and editorial handling by A. Brauer. Open access funding provided by Universitat Bern.

Author contributions—Description of the QRIN succession was undertaken by LG and MWB. LG performed the principal laboratory analyses and data interpretation. Palynological studies and interpretations were performed by MK, luminescence analyses by DM and FP, and XRF core scanning and interpretation of the results by HV. LG synthesised the data, wrote the manuscript, and prepared the figures; all authors contributed to editing the manuscript and figures. The research project was planned and supervised by FSA, GD, HM, FP and MWB.

Conflict of interest statement—No conflicts of interest have been declared by the authors.

Data availability statement

Data that support the findings of this study are available in Gegg *et al*. (2018), or further from the corresponding author upon reasonable request.

Supporting information

Additional supporting information can be found in the online version of this article.
Table S1. Palynological findings in QRIN.
Table S2. Oedometer measurement data.
Table S3. Oedometer results after Becker et al. (1987).
Table S4. Atterberg Limits from QRIN.
Table S5. Recalculated luminescence ages after Mueller et al. (2020).
information.

References

Anderson RY. 1985. Meromictic lakes and varved lake sediments in North America. US Geological Survey Bulletin, v. 1607.

Anselmetti FS, Drescher-Schneider R, Furrer H, Graf HR, Lowick SE, Preusser F, Riedi MA. 2010. A~ 180,000 years sedimentation history of a perialpine overdeepened glacial trough (Wehntal, N-Switzerland). *Swiss Journal of Geosciences* **v. 103**(no. 3): 345–361.

Autzen M, Andersen CE, Bailey M, Murray AS. in press. Calibration quartz: an update on dose calculations for luminescence dating. *Radiation Measurements* 106828.

Asselman NE, Middelkoop H. 1995. Floodplain sedimentation: quantities, patterns and processes. *Earth Surface Processes and Landforms* **v. 20**(no. 6): 481–499.

Barrett SJ, Starnberger R, Tjallingii R, Brauer A, Spötl C. 2017. The sedimentary history of the inner-alpine Inn Valley, Austria: extending the Baumkirchen type section further back in time with new drilling, *Journal of Quaternary Science* **v. 32**(no. 1): 63–79.

Barrett SJ, Drescher-Schneider R, Starnberger R, Spötl C. 2018. Evaluation of the regional vegetation and climate in the Eastern Alps (Austria) during MIS 3–4 based on pollen analysis of the classical Baumkirchen paleolake sequence. *Quaternary Research* **v. 90**(no. 1): 153–163.

Becker D, Crooks J, Been K, Jefferies M. 1987. Work as a criterion for determining in situ and yield stresses in clays. *Canadian Geotechnical Journal* **v. 24**(no. 4): 549–564.

Berner R. 1985. Sulphate reduction, organic matter decomposition and pyrite formation: Philosophical Transactions of the Royal Society of London. *Series A, Mathematical and Physical Sciences* **v. 315**(no. 1531): 25–38.

Beug H. 2004. Leitfaden der Pollenbestimmung für Mitteleuropa und angrenzende Gebiete. Verlag Dr. Friedrich Pfeil: Munich.

Bini A, Buoncristiani JF, Couterrand S, Ellwanger D, Felber M, Florineth D, Graf HR, Keller O, Kelly M, Schlüchter C. 2009. *Die Schweiz während des letzteiszeitlichen Maximums (LGM) 1:500.000*. Bundesamt für Landestopographie swisstopo:Wabern.

Bitterli-Dreher P, Graf HR, Naef H, Diebold P, Matousek F, Burger H, Pauli-Gabi T. 2007. *Geologischer Atlas der Schweiz 1:25.000. Blatt 1070 Baden*. Bundesamt für Landestopogaphie swisstopo: Wabern.

Boulton G, Paul M. 1976. The influence of genetic processes on some geotechnical properties of glacial tills. *Quarterly Journal of Engineering Geology* **v. 9**(no. 3): 159–194.

Buechi MW, Graf HR, Haldimann P, Lowick SE, Anselmetti FS. 2018. Multiple Quaternary erosion and infill cycles in overdeepened basins of the northern Alpine foreland. *Swiss Journal of Geosciences* **v. 111**: 133–167.

Burkhard M. 1990. Aspects of the large-scale Miocene deformation in the most external part of the Swiss Alps (sub-Alpine molasse to Jura fold belt). *Eclogae Geologicae Helvetiae* **v. 83**(no. 3): 559–583.

Casagrande A. 1948. Classification and identification of soils. *Transactions of the American Society of Civil Engineers* **v. 113**(no. 1): 901–930.

Dehnert A, Lowick SE, Preusser F, Anselmetti FS, Drescher-Schneider R, Graf HR, Heller F, Horstmeyer H, Kemna HA, Nowaczyk NR. 2012. Evolution of an overdeepened trough in the northern Alpine Foreland at Niederweningen, Switzerland. *Quaternary Science Reviews* **v. 34**: 127–145.

Dieleman C, Christl M, Vockenhuber C, Gautschi P, Graf HR, Akçar N. 2022. Age of the Most Extensive Glaciation in the Alps. *Geosciences* **v.12**(no. 1): 39.

Dypvik H, Harris NB. 2001. Geochemical facies analysis of fine-grained siliciclastics using Th/U, Zr/Rb and (Zr+Rb)/Sr ratios. *Chemical geology* **v. 181**(no. 1-4): 131–146.

Eisele G, Haas K, Liner S. 1994. Methode zur Aufbereitung fossilen Pollens aus minerogenen Sedimenten: Über Probleme der holozänen Vegetationsgeschichte Osttibets. *Göttinger Geographische Abhandlungen* **v. 95**: 165–166.

Evans D, Phillips E, Hiemstra J, Auton C. 2006. Subglacial till: formation, sedimentary characteristics and classification. *Earth-Science Reviews* **v. 78**(no. 1–2): 115–176.

Evans DJA. 2007. Glacial landfoms, sediments - Tills. In *Encyclopedia of Quaternary Science*, Elias S ed. Elsevier: Amsterdam; 959–975.

Eyles N, Eyles CH, Miall AD. 1983. Lithofacies types and vertical profile models; an alternative approach to the description and environmental interpretation of glacial diamict and diamictite sequences. *Sedimentology* **v. 30**(no. 3): 393–410.

Fiebig M, Herbst P, Drescher-Schneider R, Lüthgens C, Lomax J, Doppler G. 2014. Some remarks about a new Last Glacial record from the western Salzach foreland glacier basin (Southern Germany). *Quaternary International* **v. 328-329**: 107–119.

Gegg L, Buechi MW, Ebert A, Deplazes G, Madritsch H, Anselmetti FS. 2020. Brecciation of glacially overridden palaeokarst (Lower Aare Valley, northern Switzerland): result of subglacial water-pressure peaks? *Boreas* **v. 49**(no. 4): 813–827.

Gegg L, Deplazes G, Keller L, Madritsch H, Spillmann T, Anselmetti FS, Buechi MW. 2021. 3D morphology of a glacially overdeepened trough controlled by underlying bedrock geology. *Geomorphology* **v. 394**: 107950.

Gegg L, Kuster AM, Schmid D, Buechi MW. 2018. Quaternary Boreholes QBO Riniken-1 & -2 (QRIN1 & QRIN2) Data Report. Nagra Arbeitsbericht NAB 18-40.

Gaar D, Graf HR, Preusser F. 2019. New chronological constraints on the timing of Late Pleistocene glacier advances in northern Switzerland. *E&G Quaternary Science Journal* **v. 68**(no. 1): 53–73.

Graf HR. 1993. Die Deckenschotter der zentralen Nordschweiz. PhD thesis, ETH Zurich.

Graf HR. 2009a. Stratigraphie und Morphogenese von frühpleistozänen Ablagerungen zwischen Bodensee und Klettgau. *E&G Quaternary Science Journal* **v. 58**(no. 1): 12–53.

Graf HR. 2009b. Stratigraphie von Mittel-und Spätpleistozän in der Nordschweiz. *Beiträge zur Geologischen Karte der Schweiz* v. **168**.

Graf HR, Bitterli-Dreher P, Burger H, Bitterli T, Diebold P, Naef H. 2006. *Geologischer Atlas der Schweiz 1:25.000, Blatt 1070 Baden*. Bundesamt für Landestopografie swisstopo: Wabern.

Gribenski N, Valla PG, Preusser F, Roattino T, Crouzet C, Buoncristiani JF. 2021. Out-of-phase Late Pleistocene glacial maxima in the Western Alps reflect past changes in North Atlantic atmospheric circulation. *Geology* **v. 49**(no. 9): 1096–1101.

He Q, Walling D. 1998. An investigation of the spatial variability of the grain size composition of floodplain sediments. *Hydrological Processes* **v. 12**(no. 7): 1079–1094.

Holmer M, Storkholm P. 2001. Sulphate reduction and sulphur cycling in lake sediments: a review. *Freshwater Biology* **v. 46**(no. 4): 431–451.

Hughes PD, Gibbard PL, Ehlers J. 2019. The "missing glaciations" of the Middle Pleistocene. *Quaternary Research* **v. 96**: 161–183.

Huybrechts W. 2000. Post-pleniglacial floodplain sediments in Central Belgium. *Geologica Belgica* **v. 2**(no. 3-4): 29–37.

ISO. 2004. *ISO/TS 17892-5:2004. Geotechnical investigation and testing - Laboratory testing of soil - Part 5: Incremental loading oedometer test*. ISO: Geneva.

Ivy-Ochs S, Kerschner H, Reuther A, Preusser F, Heine K, Maisch M, Kubik PW, Schlüchter C. 2008. Chronology of the last glacial cycle in the European Alps. *Journal of Quaternary Science* **v. 23**(no. 6-7): 559–573.

Ivy-Ochs S, Monegato G, Reitner JM. 2022. The Alps: glacial landforms from the last glacial maximum. Palacios D, Hughes PD, Garcia-Ruiz JM, de Andres N eds. Elsevier: *European Glacial Landscapes*; 449–460.

Jordan P, Wetzel A, Reisdorf A. 2008. Swiss Jura Mountains. In *The Geology of Central Europe*, McCann T ed. Geological Society of London, 823–923.

Kamleitner S, Ivy-Ochs S, Monegato G, Gianotti F, Akçar N, Vockenhuber C, Christl M, Synal HA. 2022. The Ticino-Toce glacier system (Swiss-Italian Alps) in the framework of the Alpine Last Glacial Maximum. *Quaternary science reviews* **v. 279**: 107400.

Karlén W, Matthews JA. 1992. Reconstructing Holocene glacier variations from glacial lake sediments: studies from Nordvestlandet and Jostedalsbreen-Jotunheimen, southern Norway. Geografiska Annaler *Series A, Physical Geography* **v. 74**(no. 4): 327–348.

Kolstrup E. 1980. Climate and stratigraphy in northwestern Europe between 30,000 BP and 13,000 BP with special reference to the Netherlands. *Mededelingen Rijks Geologische Dienst* **v. 32**: 181–253.

Lang G. 1994. *Quartäre Vegetationsgeschichte Europas: Methoden und Ergebnisse*. Gustav Fischer Verlag: Jena/Stuttgart/New York.

Leonard EM. 1986. Varve studies at Hector Lake, Alberta, Canada, and the relationship between glacial activity and sedimentation. *Quaternary Research* **v. 25**(no. 2): 199–214.

Lian OB, Roberts RG. 2006. Dating the Quaternary: progress in luminescence dating of sediments. *Quaternary Science Reviews* **v. 25**(no. 19/20): 2449–2468.

Lister GS. 1984a. *Lithostratigraphy of Zübo sediments* . Contributions to Sedimentology v.**13**: 31–58.

Lister GS. 1984b. Deglaciation of the Lake Zurich area: a model based on the sedimentological record. *Contributions to Sedimentology* **v. 13**: 177–185.

Looser N, Madritsch H, Guillong M, Laurent O, Wohlwend S, Bernasconi S. 2021. Absolute age and temperature constraints on deformation along the basal décollement of the Jura fold-and-thrust belt from carbonate U-Pb dating and clumped isotopes. *Tectonics* **v. 40**(no. 3): e2020TC006439.

Lowick SE, Buechi MW, Gaar D, Graf HR, Preusser F. 2015. Luminescence dating of Middle Pleistocene proglacial deposits from northern Switzerland: methodological aspects and stratigraphical conclusions. *Boreas* **v. 44**(no. 3): 459–482.

Mailänder R, Veit H. 2001. Periglacial cover-beds on the Swiss Plateau: indicators of soil, climate and landscape evolution during the Late Quaternary. *Catena* **v. 45**(no. 4): 251–272.

Merritt JW, Connell ER, Hubbard A. 2019. Early and Middle Pleistocene environments, landforms and sediments in Scotland. *Earth and Environmental Science Transactions of the Royal Society of Edinburgh* **v. 110**(no. 1/2): 5–37.

Mills PC. 1983. Genesis and diagnostic value of soft-sediment deformation structures—a review. *Sedimentary Geology* **v. 35**(no. 2): 83–104.

Moore PD, Webb JA, Collison ME. 1991. *Pollen analysis*. Blackwell: Oxford.

Moscariello A, Schneider AM, Filippi ML. 1998. Late glacial and early Holocene palaeoenvironmental changes in Geneva Bay (Lake Geneva, Switzerland). *Palaeogeography, Palaeoclimatology, Palaeoecology* **v. 140**(no. 1-4): 51–73.

Morlock MA, Vogel H, Russell JM, Anselmetti FS, Bijaksana S. 2021. Quaternary environmental changes in tropical Lake Towuti, Indonesia, inferred from end-member modelling of X-ray fluorescence core-scanning data. *Journal of quaternary science* **v. 36**(no. 6): 1040–1051.

Mueller D, Preusser F, Buechi MW, Gegg L, Deplazes G. 2020. Luminescence properties and dating of glacial to periglacial sediments from northern Switzerland. *Geochronology* **v. 2**(no. 2): 305–323.

Naeher S, Gilli A, North RP, Hamann Y, Schubert CJ. 2013. Tracing bottom water oxygenation with sedimentary Mn/Fe ratios in Lake Zurich, Switzerland. *Chemical Geology* **v. 352**: 125–133.

Oberdorfer E. 1990. *Pflanzensoziologische Exkursionsflora*. 6th ed. Ulmer Verlag: Stuttgart.

O'Regan M, Greenwood SL, Preto P, Swärd H, Jakobsson M. 2016. Geotechnical and sedimentary evidence for thick-grounded ice in southern Lake Vättern during deglaciation. *GFF* **v. 138**(no. 2): 355–366.

Penck A, Brückner E. 1909. *Die Alpen im Eiszeitalter*. Tauchnitz Verlag: Leipzig.

Pisarska-Jamrozy M, Weckwerth P. 2013. Soft-sediment deformation structures in a Pleistocene glaciolacustrine delta and their implications for the recognition of subenvironments in delta deposits. *Sedimentology* **v. 60**(no. 3): 637–665.

Preusser F, Schlüchter C. 2004. Dates from an important early Late Pleistocene ice advance in the Aare valley, Switzerland. *Eclogae Geologicae Helvetiae* **v. 97**: 245–253.

Preusser F, Drescher-Schneider R, Fiebig M, Schlüchter C. 2005. Reinterpretation of the Meikirch pollen record, Swiss Alpine Foreland, and implications for Middle Pleistocene chronostratigraphy. *Journal of Quaternary Science* **v. 20**(no. 6): 607–620.

Preusser F, Graf HR, Keller O, Krayss E, Schlüchter C. 2011. Quaternary glaciation history of northern Switzerland. *E&G Quaternary Science Journal* **v. 60**: 282–305.

Pugin A, Bezat E, Weidmann M, Wildi W. 1993. Le bassin d'Ecouteaux (Vaud, Suisse): Témoin de trois cycles glaciaires quaternaires. *Eclogae Geologicae Helvetiae* **v. 86**(no., 2): 343–354.

Qi J, Vermeer PA, Cheng G. 2006. A review of the influence of freeze-thaw cycles on soil geotechnical properties. *Permafrost and periglacial processes* **v. 17**(no. 3): 245–252.

Raab T, Laeopold M, Völkel J. 2007. Character, age, and ecological significance of Pleistocene periglacial slope deposits in Germany. *Physical Geography* **v. 28**(no. 6): 451–473.

Regnéll C, Haflidason H, Mangerud J, Svendsen JI. 2019. Glacial and climate history of the last 24 000 years in the Polar Ural Mountains, Arctic Russia, inferred from partly varved lake sediments. *Boreas* **v. 48**(no. 2): 432–443.

Rickard D, Mussmann M, Steadman JA. 2017. Sedimentary sulfides. *Elements* **v. 13**(no. 2): 117–122.

Schlüchter C. 1984. Geotechnical properties of Zübo-sediments. *Contributions to Sedimentology* **v. 13**: 135–140.

Schlüchter C. 1989. Thalgut: ein umfassendes eiszeitstratigraphisches Referenzprofil im nördlichen Alpenvorland. *Eclogae Geologicae Helvetiae* **v. 82**(no. 1): 277–284.

Schlüchter C. 1997. Sedimente des Gletschers (Teil I). Bulletin für angewandte Geologie, **v. 2**(no. 2): 99-112.

Schlüchter C, Akçar N, Ivy-Ochs S. 2021. The Quaternary Period in Switzerland, *Landscapes and Landforms of Switzerland*. Springer, 47–69.

Schultheiss P, Weaver P. 1992. Multi-sensor core logging for science and industry. *Proceedings OCEANS'92 Mastering the Oceans Through Technology v*. **2**: 608-613.

Schwenk MA, Schläfli P, Bandou D, Gribenski N, Douillet GA, Schlunegger F. 2022. *From glacial erosion to basin overfill: a*

240 m-thick overdeepening–fill sequence in Bern. Scientific Drilling v.**30**: 17–42.

Seguinot J, Ivy-Ochs S, Jouvet G, Huss M, Funk M, Preusser F. 2018. Modelling last glacial cycle ice dynamics in the Alps. *The Cryosphere* **v. 12**(no. 10): 3265–3285.

Sidler C. 1984. Palynological investigations of Zübo sediments. *Contributions to Sedimentology* **v. 13**: 103–114.

Starnberger R, Drescher-Schneider R, Reitner JM, Rodnight H, Reimer PJ, Spötl C. 2013. Late Pleistocene climate change and landscape dynamics in the Eastern Alps: the inner-alpine Unterangerberg record (Austria). *Quaternary Science Reviews* **v. 68**: 17–42.

Starnberger R, Rodnight H, Spötl C. 2011. Chronology of the last glacial maximum in the Salzach Palaeoglacier area (Eastern Alps). *Journal of Quaternary Science* **v. 26**(no. 5): 502–510.

Suits NS, Wilkin RT. 1998. Pyrite formation in the water column and sediments of a meromictic lake. *Geology* **v. 26**(no. 12): 1099–1102.

Svendsen JI, Færseth LMB, Gyllencreutz R, Haflidason H, Henriksen M, Hovland MN, Lohne ØS, Mangerud J, Nazarov D, Regnéll C. 2019. Glacial and environmental changes over the last 60 000 years in the Polar Ural Mountains, Arctic Russia, inferred from a high-resolution lake record and other observations from adjacent areas. *Boreas* **v. 48**(no. 2): 407–431.

Tierney JE, Poulsen CJ, Montañez IP, Bhattacharya T, Feng R, Ford HL, Hönisch B, Inglis GN, Petersen SV, Sagoo N. 2020. Past climates inform our future. *Science* **v. 370**(no): 6517.

Trenter N. 1999. Engineering in glacial tills, CIRIA Report C504. Construction Research and Information Association: London.

Urban B, Bigga G. 2015. Environmental reconstruction and biostratigraphy of late Middle Pleistocene lakeshore deposits at Schöningen. *Journal of Human Evolution* **v. 89**: 57–70.

Van der Meer JJ, Kjær KH, Krüger J, Rabassa J, Kilfeather A. 2009. Under pressure: clastic dykes in glacial settings. *Quaternary Science Reviews* **v. 28**(no. 7-8): 708–720.

Van Dijk D, Hobday DK, Tankard A. 1978. *Permo-Triassic Lacustrine Deposits in the Eastern Karoo Basin, Natal, South Africa*, Matter A, Tucker ME eds. Modern and ancient lake sediments, 225–239.

Van Gelder G, de Graaff L, Schurink E. 1990. Subglacial consolidation of fine-grained stratified sediments: a neglected tool in reconstructing ice-thickness in Pleistocene valley glaciers. *Arctic and Alpine Research*: 329–340.

Van Husen D, Reitner JM. 2011. An outline of the Quaternary stratigraphy of Austria. *E&G Quaternary Science Journal* **v. 60**(no. 2/3): 366–387.

Veit H, Trauerstein M, Preusser F, Messmer T, Gnägi C, Zech R, Wüthrich L. 2017. Late Glacial/Early Holocene slope deposits on the Swiss Plateau: Genesis and palaeo-environment. *Catena* **v. 158**: 102–112.

Vogel H, Wagner B, Zanchetta G, Sulpizio R, Rosén P. 2010. A paleoclimate record with tephrochronological age control for the last glacial-interglacial cycle from Lake Ohrid, Albania and Macedonia. *Journal of Paleolimnology* **v. 44**(no. 1): 295–310.

VSS. 2008. SN 670 345b. Böden – Konsistenzgrenzen. VSS: Zurich.

Welten M. 1982. Stand der palynologischen Quartärforschung am schweizerischen Nordalpenrand. *Geographica Helvetica* **v. 37**(no. 2): 75–83.

Wennrich V, Minyuk P, Borkhodoev V, Francke A, Ritter B, Nowaczyk NR, Sauerbrey M, Brigham-Grette J, Melles M. 2014. Pliocene to Pleistocene climate and environmental history of Lake El'gygytgyn, Far East Russian Arctic, based on high-resolution inorganic geochemistry data. *Climate of the Past* **v. 10**(no. 4): 1381–1399.

Wyssling L, Wyssling G. 1978. Interglaziale See-Ablagerungen in einer Bohrung bei User (Kanton Zürich). *Eclogae Geologicae Helvetiae* **v. 71**(no. 2): 357–375.

Żarczyński M, Wacnik A, Tylmann W. 2019. Tracing lake mixing and oxygenation regime using the Fe/Mn ratio in varved sediments: 2000 year-long record of human-induced changes from Lake Żabińskie (NE Poland). *Science of the Total Environment* **v. 657**: 585–596.

Ziegler PA, Fraefel M. 2009. Response of drainage systems to Neogene evolution of the Jura fold-thrust belt and Upper Rhine Graben. *Swiss Journal of Geosciences* **v. 102**(no. 1): 57–75.

Zolitschka B, Francus P, Ojala AE, Schimmelmann A. 2015. Varves in lake sediments–a review. *Quaternary Science Reviews* **v. 117**: 1–41.

Table S1: Palynological findings in QRIN, concentrations in grains per 1 cm^3. g & s = grasses and sedges / (+) = few / + = some / ++ = many / +++ = very many / *cf.* = not unequivocally identifiable.

34.75	**30.58**	**25.90**	**21.39**	**16.58**	**14.49**	**10.80**	**6.90**	**Sample depth [m]**	
2	6	8.5	97	335.5	392.5	485.5	466	**Counted grains**	
	0.5	1.5	18	69	64	51	56	***Pinus***	Arboreal taxa
			2	1	8	2		***Pinus cembra* type**	Arboreal taxa
1		1	2	3	2	18	13	***Betula***	Arboreal taxa
				2	2	43	9	***Betula cf. nana* type**	Arboreal taxa
			1	1	2	4	1	***Salix***	Arboreal taxa
						1		***Alnus viridis* type**	Arboreal taxa
			1	1	3		1	***Juniperus***	Arboreal taxa
			1	1		4	1	***Hippophae***	Arboreal taxa
				3	1	1	2	***Ephedra distachya* type**	Arboreal taxa
				2				***Ephedra fragilis* type**	Arboreal taxa
	1							***Corylus***	Arboreal taxa, likely reworked
					cf.		1	***Quercus***	Arboreal taxa, likely reworked
	1			2			4	***Alnus glutinosa* type**	Arboreal taxa, likely reworked
	1.5	3.5	2.5	4.5	5	*cf.*		***Picea***	Arboreal taxa, likely reworked
	1	1.5		1	1			***Abies***	Arboreal taxa, likely reworked
1	1	1	17	59	54	160	53	**Poaceae**	G & s
			37	151	189	122	138	**Cyperaceae**	G & s
			4	7	15	8	53	***Artemisia***	Non-arboreal taxa
			2	8	7	2	15	***Chenopodiaceae***	Non-arboreal taxa
				2	3	20	16	***Helianthemum***	Non-arboreal taxa
				2	4	6	4	***Saxifraga aizoides* group**	Non-arboreal taxa
			3	8	6	6	23	***Thalictrum***	Non-arboreal taxa
			2	1	2	2	8	**Caryophyllaceae**	Non-arboreal taxa
							1	***Cerastium* type**	Non-arboreal taxa
						3	2	***Gipsophila***	Non-arboreal taxa
				1			1	***Silene* type**	Non-arboreal taxa
						1		**Plumbaginaceae**	Non-arboreal taxa
						3	4	**Rubiaceae**	Non-arboreal taxa
						1		***Plantago tenuiflora* type**	Non-arboreal taxa
			1		1	2		***Plantago sp.***	Non-arboreal taxa
				1	3	1	3	***Achillea* type**	Non-arboreal taxa
						1	2	***Solidago* type**	Non-arboreal taxa
			2	4	5	3	5	**Cichoriaceae**	Non-arboreal taxa
				1	4	4	7	**Brassicaceae**	Non-arboreal taxa
						1		**Apiaceae**	Non-arboreal taxa
						1		**Rosaceae**	Non-arboreal taxa
							1	**Ranunculaceae**	Non-arboreal taxa
							1	***Ranunculus* type**	Non-arboreal taxa
						1		***Valeriana***	Non-arboreal taxa
			1			2	2	***Botrychium***	Non-arboreal taxa
				1	9	11	28	***Selaginella selaginoides***	Non-arboreal taxa
			1		3	1	11	**Varia**	
(+)	+	+	+++	+	+	+	++	**Indeterminata**	
							1	***Sparganium* type**	Aquatic taxa
				1				***cf. Batrachium* type**	Aquatic taxa
						4		***cf. Triglochin***	Aquatic taxa
			1					***Pediastrum***	Aquatic taxa
			1	7	2	1	2	***Botryococcus***	Aquatic taxa
					1			**Monolete spores**	Aquatic taxa
				1			1	***Sphagnum***	Aquatic taxa
(+)	(+)	+	+++	++	+	+	++	**Pre-Quaternary taxa**	Aquatic taxa
(+)		+		+	+	++	++	**Pre-Quat. marine taxa**	Aquatic taxa
16	**68**	**142**	**414**	**1286**	**1768**	**7223**	**2583**	**Terrestrial pollen per cm^3**	
50.0	**83.3**	**88.2**	**27.8**	**26.7**	**22.3**	**25.4**	**18.9**	**Arboreal taxa [%]**	

Table S2: Oedometer measurement data (sample compaction in response to applied vertical load) and work done per unit volume after Becker *et al.* (1987). Initial thickness of all samples is 20 mm ([1]: 19.1 mm).

Sample and depth	**OED-1** [1] **9.65 m**		**OED-2 16.26 m**		**OED-3** [2] **20.89 m**		**OED-4** [2] **29.15 m**		**OED-5 31.88 m**	
Load [kN/m²]	**Compact. [mm]**	**Δ Work [kN/m]**	**Compact. [mm]**	**Δ Work [kN/m]**	**Compact. [mm]**	**Δ Work [kN/m]**	**Compact. [mm]**	**Δ Work [kN/m]**	**Compact. [mm]**	**Δ Work [kN/m]**
12.5	0.39	-	-	-	0.09	-	0.09	-	0.19	-
25	0.57	188	0.34	-	0.15	57	0.17	75	0.28	85
50	0.79	480	0.43	194	0.27	233	0.40	44	0.42	270
100	1.06	1240	0.64	829	0.45	687	0.73	1269	0.61	776
200 ([2] 175)	1.36	2984	0.83	1466	0.68	1695	1.09	2928	0.86	1863
300 ([2] 275)	-	-	0.96	1983	0.84	2109	-	-	1.01	2275
400 ([2] 375)	1.70	7387	1.08	2835	0.96	2682	1.52	7134	1.10	2383
600	-	-	1.32	7790	1.23	8045	-	-	1.32	7261
800	2.11	19355	1.54	11419	1.41	9380	2.03	17712	1.49	9603
1200	-	-	1.94	28210	1.74	23055	-	-	1.66	14911
1600	-	-	2.24	37817	1.98	30622	2.59	41086	1.81	22357
2400	-	-	2.72	82253	2.40	67253	-	-	2.08	47500
3200	-	-	3.01	106820	2.67	89902	3.18	92312	2.26	61577

Table S3: Oedometer results after Becker *et al.* (1987) compared to the estimated present-day sediment overload.

Sample	Depth [m]	Sed. overload [kN/m^2]	Prec. pressure [kN/m^2]
OED-1	9.65	~130	312 (+ 133 %)
OED-2	16.26	~200	751 (+ 270 %)
OED-3	20.89	~250	909 (+ 259 %)
OED-4	29.15	~340	1218 (+ 256 %)
OED-5	31.88	~370	594 (+ 61 %)

Table S4: Atterberg Limits from QRIN. WC = natural water content, LL = liquid limit, PL = plastic limit.

Sample	Depth [m]	WC	LL	PL
ATL-1	9.65	25 %	25 %	14 %
ATL-2	16.26	23 %	34 %	17 %
ATL-3	20.89	22 %	34 %	16 %
ATL-4	29.15	20 %	24 %	16 %
ATL-5	31.88	21 %	31 %	14 %
ATL-6	39.88	9 %	18 %	13 %

Table S5: Recalculated luminescence ages after Mueller *et al.* (2020), original ages are given in brackets.

Sample	Depth [m]	LFA	Quartz age [ka]	Feldspar age [ka]	Polymineral age [ka]
RIN1	4.12	5	212 ± 12 (177 ± 11)	190 ± 8 (165 ± 7)	-
RIN2	6.12	5	198 ± 14 (169 ± 10)	192 ± 10 (167 ± 8)	-
RIN3	6.34	5	205 ± 12 (180 ± 11)	185 ± 9 (162 ± 8)	-
RIN4	9.04	4d	186 ± 10 (164 ± 9)	183 ± 8 (160 ± 7)	-
RIN5	10.25	4c	-	-	159 ± 8 (138 ± 7)
RIN6	16.55	4c	-	-	194 ± 10 (169 ± 9)
RIN8	29.63	4b	>187 ± 15 (>163 ± 13)	-	-
RIN13	35.37	3	>210 ± 29 (>183 ± 26)	-	-